Contribution from the Departments of Chemistry, Indiana University, Bloomington, Indiana 47405, and The Ohio State University, Columbus, Ohio 43210

Metal-Metal Bonds Involving the f Elements. 4.[1] Molecular Orbital Studies of Metal-Metal and Metal-Ligand Interactions in Dinuclear Uranium(V) Systems

Roger H. Cayton,[2a] Kevin J. Novo-Gradac,[2b] and Bruce E. Bursten*[,2b]

Received November 9, 1990

The electronic structures of a series of dinuclear uranium(V) complexes have been investigated using Xα-SW molecular orbital calculations including quasirelativistic corrections. Complexes of the formula U_2H_{10} and $U_2(OH)_{10}$ were used to model the metal-ligand σ and π interactions, respectively, in the known species $U_2(O\text{-}i\text{-}Pr)_{10}$. Two basic geometries were investigated: a vertex-sharing bioctahedron with only terminal ligands (D_{4h} symmetry) and an edge-sharing bioctahedron containing two bridging ligands (D_{2h} symmetry). The latter geometry, which is that of $U_2(O\text{-}i\text{-}Pr)_{10}$, was also examined at U-U bonding and nonbonding distances. The calculations indicate that the U-U interactions are significantly perturbed when H is replaced by OH, owing to strong donation from the OH pπ orbitals into selected U 5f orbitals. The result is a lack of any appreciable U-U interaction for $U_2(OH)_{10}$ in either the D_{4h} or D_{2h} geometry. In addition, the overall OH π donation to the U 5f levels is enhanced in the D_{2h} geometry. The electronic structure of a hypothetical U(V) dimer, $Cp_2U_2O_4$, was also examined in both bridged and unsupported geometries. The unbridged geometry, like that for $U_2(OH)_{10}$, suffered from a destabilization of the U-U σ orbital due to ligand π donation and revealed no net U-U bonding. However, the geometry exhibiting two bridging oxo ligands maintains the U-U σ-bonding MO as its lowest energy U 5f orbital.

Introduction

The transition metals display a marked proclivity for the formation of strong metal-metal bonds.[3] For example, each member of the group 6 transition metals (Cr, Mo, W) forms complexes exhibiting metal-metal bond orders ranging from one to four, with a variety of supporting ligands. By contrast, the corresponding group 6 actinide element, uranium, shows no capability for participation in metal-metal bonding; in fact, the preparation of a discrete molecular compound that contains a direct metal-metal bond between two actinide elements is a goal that has long eluded actinide chemists. It is not obvious to us that the inclusion of valence f orbitals on a metal should preclude metal-metal bond formation. For example, in our previous study of the metal-metal bonding in actinide-transition-metal heterobimetallic complexes we found that the actinide 6d orbitals were more important than the 5f orbitals for metal-metal bond formation.[4] Our earlier[5] and more recent[1] studies of the bonding in U_2 indicate a high likelihood of U-U bond formation in this "naked" dimer, although the importance of 6d vs 5f participation is still open to question.

Recently, Cotton and co-workers successfully prepared and structurally characterized a series of bimetallic uranium complexes, including $U_2(OR)_{10}$ (**1**; R = $CHMe_2$).[6] The X-ray crystal

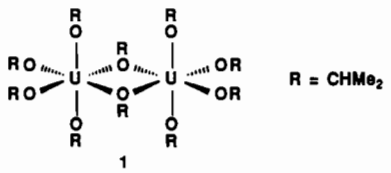

1

structure of this compound reveals several interesting features. The overall geometry is essentially that of an edge-sharing bioctahedron. The U···U distance, 3.789 Å, is long, leading to a distortion of the central U_2O_2 core: Whereas an idealized edge-sharing bioctahedron would exhibit M-(μ-L)-M and (μ-L)-M-(μ-L) angles of 90°,[7] the U-(μ-O)-U and (μ-O)-U-(μ-O) angles in **1** are 111.4 and 68.6°, respectively. This distortion may be due to a repulsive interaction between the U atoms or to more subtle effects involving the μ-OR ligands and the uranium valence orbitals. A second interesting structural feature of **1** is that the U-O-C angles of the terminal alkoxide ligands vary from 160 to 176°, suggesting nearly sp hybridization of the oxygen atoms. Nearly linear M-O-C angles have been noted previously for other actinide alkoxide complexes, such as $U(OMe)_6$.[8]

These two structural features differ markedly from those observed in isoelectronic transition-metal systems.[7] For example, d^1-d^1 edge-sharing bioctahedral transition-metal complexes that contain both terminal and bridging alkoxide ligands display M_2O_2 cores indicative of a M-M single bond and much more acute M-(t-O)-C angles (135-145°).[9] This trend is also apparent in the recently characterized homoleptic methoxide complexes $W_2(OMe)_{10}$ (d^1-d^1) and $Re_2(OMe)_{10}$ (d^2-d^2).[10] These edge-sharing bioctahedral systems exhibit metal-metal bond lengths consistent with single and double bonds, respectively, and demonstrate a remarkable electronic interplay of the methoxide π orbitals with the metal-metal bonding orbitals. In view of these results from transition-metal chemistry, it is very striking that **1** does *not* contain a U-U bond, and we believe that the actinide valence f orbitals must play an important role in the structure and bonding of the U(V)-U(V) bimetallic systems.

In an effort to understand better the lack of metal-metal bonding in dinuclear actinide complexes, we have used Xα-SW molecular orbital calculations[11] with quasirelativistic corrections[12] to investigate the electronic structure of a series bimetallic U(V)-U(V) complexes. In order to examine the degree of f-orbital participation in both metal-ligand and metal-metal interactions, a variety of ligand sets and geometries were considered. We begin by considering a model uranium(V) hydride complex, U_2H_{10}. From its electronic structure, the "σ-only" effects of the ligands can be extracted, and the extent of metal-metal interaction can be examined in the absence of ligand π effects. The hydride ligands will then be replaced by hydroxide ligands to model the known alkoxide dimers. Such a procedure allows us to investigate directly the extent of ligand π- to metal f-orbital interaction and its influence on metal-metal bonding. Finally, the model system

(1) Part 3: Pepper, M.; Bursten, B. E. *J. Am. Chem. Soc.* **1990**, *112*, 7803-7804.
(2) (a) Indiana University. (b) The Ohio State University.
(3) (a) Cotton, F. A.; Wilkinson, G. *Advanced Inorganic Chemistry*, 5th ed.; Wiley: New York, 1988; pp 1052-1096. (b) Cotton, F. A.; Walton, R. A. *Multiple Bonds Between Metal Atoms*; Wiley: New York, 1982. (c) Cotton, F. A.; Chisholm, M. H. *Chem. Eng. News* **1982**, *60* (June 28), 40-54.
(4) Bursten, B. E.; Novo-Gradac, K. J. *J. Am. Chem. Soc.* **1987**, *109*, 904-905.
(5) Bursten, B. E.; Ozin, G. A. *Inorg. Chem.* **1984**, *23*, 2910-2911.
(6) Cotton, F. A., Marler, D. O.; Schwotzer, W. *Inorg. Chem.* **1984**, *23*, 4211-4215.
(7) Cotton, F. A. *Polyhedron* **1987**, *6*, 667-677 and references therein.
(8) (a) Bursten, B. E.; Casarin, M.; Ellis, D. E.; Fragalà, I.; Marks, T. J. *Inorg. Chem.* **1986**, *25*, 1257-1261. (b) Sattelberger, A. P.; Van Der Sluys, W. G. *Chem. Rev.* **1990**, *90*, 1027-1040.
(9) (a) Cotton, F. A.; Diebold, M. P.; Roth, W. *Inorg. Chem.* **1985**, *24*, 3509. (b) Chisholm, M. H.; Kirkpatrick, C. C.; Huffman, J. C. *Inorg. Chem.* **1981**, *20*, 871. (c) Cotton, F. A.; DeMarco, D.; Kolthammer, B. W. S.; Walton, R. A. *Inorg. Chem.* **1981**, *20*, 3048-3051. (d) Barder, T. J.; Cotton, F. A.; Lewis, D.; Schwotzer, W.; Tetrick, S. M.; Walton, R. A. *J. Am. Chem. Soc.* **1984**, *106*, 2882-2891.
(10) Bryan, J. C.; Wheeler, D. R.; Clark, D. L.; Huffman, J. C.; Sattelberger, A. P. *J. Am. Chem. Soc.*, in press.
(11) Case, D. A. *Annu. Rev. Phys. Chem.* **1982**, *33*, 151-171.
(12) Wood, J. H.; Boring, A. M. *Phys. Rev. B* **1978**, *18*, 2701-2711.

0020-1669/91/1330-2265$02.50/0

Table I. Energies and Percent Character of the Valence Orbitals of **2a**

MO	ϵ, eV	% U	% s	% p	% d	% f	% H	type[a]
$4e_g$	−0.67	90		8	8	84	10	ϕ^*/π^*
$4a_{2u}$	−0.85	96	0	4	1	95	4	σ^*
$4e_u$	−1.52	97		6	11	83	3	ϕ/π
$3e_g$	−1.85	100		0	1	99	0	π^*/ϕ^*
$2b_{2u}$	−1.86	100			0	100	0	δ^*
$1b_{1u}$	−1.89	100			0	100	0	δ^*
$2b_{1g}$	−2.19	100			0	100	0	δ
$1b_{2g}$	−2.23	100			1	99	0	δ
$3e_u$	−2.44	100		1	6	93	0	π/ϕ
$4a_{1g}$[b]	−2.81	100	3	1	7	89	0	σ
$2e_g$	−5.07	56		18	0	82	44	
$2e_u$	−5.56	54		18	0	82	46	
$3a_{2u}$	−5.82	44	22	19	12	47	56	
$3a_{1g}$	−6.70	44	41	5	37	17	56	
$2a_{2u}$	−7.41	38	34	2	58	6	62	
$2a_{1g}$	−8.14	40	21	0	79	0	60	
$1b_{2u}$	−8.19	39			100	0	61	
$1b_{1g}$	−8.68	40			100	0	60	

[a] Refers to U–U interaction type for the primarily 5f-based orbitals. [b] Highest occupied molecular orbital.

$Cp_2U_2O_4$ is considered, in an attempt to devise a ligand set that may promote actinide–actinide bond formation.

Results and Discussion

U_2H_{10}. The model σ-only system U_2H_{10} (**2**) was examined in two assumed geometries. One contains only terminal hydride ligands and has D_{4h} symmetry (**2a**), while the other is a D_{2h}

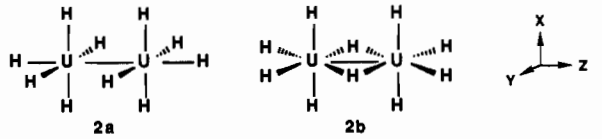

edge-sharing bioctahedron with two bridging hydride ligands (**2b**). These geometries are illustrated along with the coordinate system used. In both model geometries, a U–U distance of 2.84 Å was assumed, which we believe is representative of a U–U single bond.[13] In both geometries, the uranium atoms are in pseudooctahedral ligand fields. We will begin by analyzing the D_{4h} complex **2a**, as the lack of bridging ligands significantly simplifies its bonding description.

The valence MOs of **2a** are depicted on the left side of Figure 1. The orbitals are split into two sets, the lower set comprising the U–H bonding levels and the upper set representing the metal, primarily 5f, orbitals. Under O_h symmetry, the f orbitals are best described as metal–ligand σ (f_{z^3}, f_{y^3}, and f_{x^3}), π ($f_{z(x^2-y^2)}$, $f_{x(z^2-y^2)}$, and $f_{y(z^2-x^2)}$), and δ (f_{xyz}) orbitals. These three sets of orbitals are bases for the t_{1u}, t_{2u}, and a_{2u} representations, respectively.[14] Therefore, in addition to the usual d^2sp^3 metal hybridization in an octahedral field, the t_{1u} 5f orbitals can also contribute to the metal–ligand σ bonding. The actual contribution of the individual atomic orbitals to the octahedral field hybridization will, of course, be dependent on their relative energies and radial extension. Table I lists the energies and the compositions of the valence orbitals of **2a**. Only the four uppermost U–H bonding levels contain appreciable f character. The metal character of the highest two of these ($2e_u$ and $2e_g$) are dominated by f character (82%) and represent bonding interactions between the f_{z^3} and f_{y^3} combinations and the hydride ligands. The other two orbitals ($3a_{1g}$ and $3a_{2u}$) contain significantly less f character, which is present as f_{z^3} U–U σ and σ^* combinations. Summation of the total contribution of s, p, d, and f character in the U–H bonding orbitals yields a hybridization scheme that is best described as f^2d^2sp.

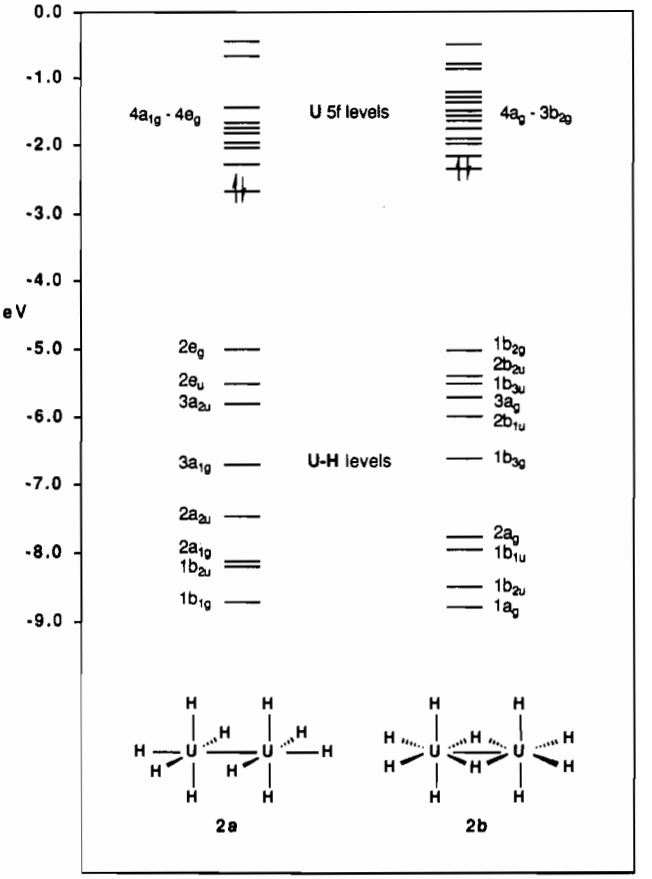

Figure 1. Molecular orbital diagram of the valence orbitals of the model complexes **2a** (left) and **2b** (right) through the U 5f-based levels.

The orbital splitting within the uranium 5f block is due primarily to metal–metal interaction, and in accord with intuition, the lowest energy metal-based orbital represents a U–U σ-bonding interaction. This $4a_{1g}$ orbital, which is the HOMO of the complex, is nearly pure U $5f_{z^3}$ in character and is stabilized 0.32 eV below the $3e_u$ LUMO.[15]

This electronic description of **2a** can readily be extended to the D_{2h} model complex, **2b**, in which two of the hydrides now occupy bridging positions. As in **2a**, each uranium atom in **2b** is in a pseudooctahedral environment. For this reason, the metal–ligand orbitals of **2b** can essentially be derived from those of **2a** by

(13) In the α form of uranium metal, the average nearest-neighbor U–U distance to the four nearest neighbors is 2.8 Å: (a) Jacob, C. W.; Warren, B. E. *J. Am. Chem. Soc.* **1937**, *59*, 2588–2591. (b) Sturcken, E. F. *Acta Crystallogr.* **1960**, *13*, 852.

(14) For a discussion of the transformation of the standard f orbitals to an octahedral field, see: Cotton, F. A. *Chemical Applications of Group Theory*, 3rd ed.; Wiley: New York, 1990; p 441–442.

(15) It should be noted that the U–U orbitals of π and ϕ symmetry mix under D_{4h} symmetry to form π/ϕ hybrid orbitals. The $3e_u$ LUMO is one of these hybrid orbitals.

Table II. Energies and Percent Characters of the Valence Orbitals of **2b**

MO	ϵ, eV	% U	% s	% p	% d	% f	% H	type[a]
$3b_{2g}$	−0.65	93		7	9	84	7	ϕ^*/π^*
$3b_{3g}$	−0.95	98		2	2	96	2	π^*/ϕ^*
$5a_g$	−0.98	97	2	3	26	72	3	δ/σ
$4b_{1u}$	−1.35	99	1	1	2	96	0	σ^*/δ^*
$3b_{1u}$	−1.44	100	1	0	3	96	0	δ^*/σ^*
$3b_{3u}$	−1.51	99		4	10	86	1	ϕ/π
$2b_{2g}$	−1.60	100		0	1	98	0	π^*/ϕ^*
$1a_u$	−1.63	100			1	99	0	δ^*
$4b_{2u}$	−1.65	99		0	1	99	1	π/ϕ
$2b_{3g}$	−1.73	100		0	0	100	0	π^*/ϕ^*
$3b_{2u}$	−1.98	99		0	1	99	1	π/ϕ
$1b_{1g}$	−1.99	100			1	99	0	δ
$2b_{3u}$	−2.25	100		1	10	89	0	π/ϕ
$4a_g$[b]	−2.40	99	0	1	6	92	0	σ/δ
$1b_{2g}$	−5.13	53		22	0	78	47	
$2b_{2u}$	−5.49	47		27	1	72	53	
$1b_{3u}$	−5.65	52		21	0	78	48	
$3a_g$	−5.86	47	2	12	8	77	53	
$2b_{1u}$	−6.05	41	32	24	9	36	59	
$1b_{3g}$	−6.77	44		15	53	32	56	
$2a_g$	−7.85	32	98	0	2	0	68	
$1b_{1u}$	−8.03	38	14	1	84	2	62	
$1b_{2u}$	−8.58	38		0	100	0	62	
$1a_g$	−8.78	40	0	0	99	1	60	

[a] Refers to U–U interaction type for the primarily 5f-based orbitals. [b] Highest occupied molecular orbital.

rotation of each of the UH_5 fragments through 45° about the x axis. The valence MO diagram of **2b** is shown on the right side of Figure 1, and the energies and compositions of the orbitals are given in Table II. An examination of the distribution of metal character in the U–H bonding levels ($1a_g$–$1b_{2g}$) again leads to a hybridization scheme best described as f^2d^2sp. Like in the case of D_{4h} geometry, the U–H bonding orbitals that contain significant f character are the highest energy ones. The metal–metal interaction within the f block becomes, as expected, more complicated in the D_{2h} geometry. In addition to the π/ϕ mixing, the U–U σ interaction can now mix with one of the U–U δ combinations. This interaction serves to weaken the σ interaction, as demonstrated by the 1.05-eV splitting of the primarily σ/σ^* set ($4a_g$, $4b_{1u}$) of **2b** as compared to the 1.96-eV splitting of the σ/σ^* set ($4a_{1g}$, $4a_{2u}$) of **2a**. Hence, the somewhat weak U–U interaction in the D_{4h} case is further diminished in the change to the D_{2h} geometry. It is important to note, however, that the σ-only ligand set in both **2a** and **2b** only slightly perturbs the f block and the metal–metal $\sigma < \pi < \delta$ manifold remains essentially intact in the lower f levels. Replacement of the σ-only hydride set with the π-donor hydroxide set will provide a measure of the involvement of the f block with ligand π orbitals.

$U_2(OH)_{10}$. The model alkoxide system $U_2(OH)_{10}$ (**3**) was also examined in two basic geometries. The first of these is an all terminal D_{4h} geometry (**3a**), which is analogous to structure **2a**.

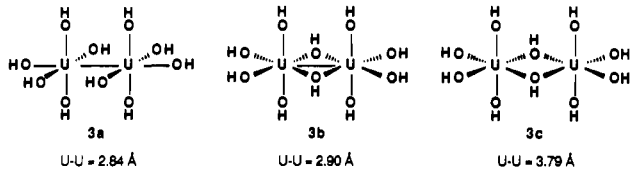

The second geometry is a bis-bridged D_{2h} one, which was examined at both a short U–U distance (2.90 Å), **3b**, and a long U–U distance (3.79 Å), **3c**. In all cases, the terminal OH ligands were constrained to be linear. These model systems will allow us to evaluate the electronic perturbations resulting from the hydroxide π orbitals in both unsupported and bridged conformations.

Once again we will begin with the less complicated D_{4h} complex, **3a**. The frontier molecular orbital diagram of **3a** is depicted on the left half of Figure 2. Three distinct orbital groups are found, corresponding, in increasing energy, to the U–OH σ- and π-bonding levels and the U f block, respectively. Tables III and IV list the energies and compositions of the U f block and U–O π orbitals of **3a**. Focusing first on the U f block (Table III) allows

Table III. Energies and Percent Characters of the f-Block Orbitals of **3a**

MO	ϵ, eV	type[a]	% U	% OH
$8e_g$	−5.38	ϕ^*/π^*	86	14
$8e_u$	−5.61	ϕ/π	86	14
$7a_{2u}$	−5.64	σ^*	89	11
$4b_{2u}$	−6.32	δ^*	86	14
$7e_g$	−6.38	π^*/ϕ^*	89	11
$4b_{1g}$	−6.51	δ	88	12
$7e_u$	−6.89	π/ϕ	88	12
$7a_{1g}$	−7.07	σ	90	10
$2b_{1u}$	−7.09	δ^*	100	0
$2b_{2g}$	−7.33	δ	100	0

[a] Refers to U–U interaction type.

Table IV. Energies and Percent Characters of the U–O π Orbitals of **3a**

MO	ϵ, eV	% U	% f	% d	% p	% s	% OH
$6e_g$	−9.65	3	66	3	31	0	97
$1a_{1u}$	−9.83	0	0	0	0	0	100
$1a_{2g}$	−9.95	0	0	0	0	0	100
$6e_u$	−9.95	6	63	2	35	0	94
$6a_{2u}$	−10.13	8	58	2	39	1	92
$5e_g$	−10.56	11	63	8	29	0	89
$3b_{2u}$	−10.58	18	100	0	0	0	82
$5e_u$	−10.81	15	89	1	10	0	85
$4e_g$	−10.99	13	51	48	1	0	87
$6a_{1g}$	−11.03	13	75	7	14	4	87
$3b_{1g}$	−11.28	17	100	0	0	0	83
$1b_{1u}$	−11.53	10	0	100	0	0	90
$4e_u$	−11.59	11	3	97	0	0	89
$1b_{2g}$	−11.77	11	0	100	0	0	89

several interesting features to become apparent. The U–U hybridization is essentially the same as that detailed earlier for the σ-only model, **2a**. However, in contrast to the intuitive U–U splitting ($\sigma < \pi < \delta$) observed in the σ-only system, the ordering of the U–U orbitals in **3a** is significantly perturbed by the ligands. In fact, the lowest two orbitals are the U–U δ ($2b_{2g}$) and δ^* ($2b_{1u}$) orbitals, which are the only metal-based orbitals that do not contain significant OH character; antibonding interactions with the OH π orbitals destabilizes the other 5f orbitals, yielding the nonintuitive ordering. A correlation of the U-based orbitals of **2a** to those of **3a** is given in Figure 3.

The U–U δ and δ^* orbitals are unable to interact with the OH π group orbitals of b_{2g} and b_{1u} symmetry because the latter lie

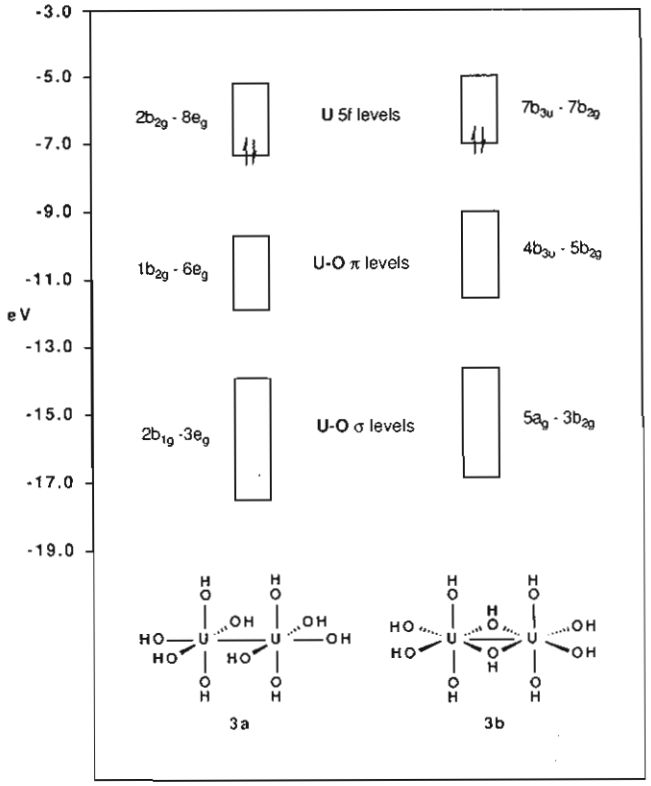

Figure 2. Molecular orbital diagram displaying the blocks of valence orbitals of the model complexes **3a** (left) and **3b** (right) through the U 5f-based levels.

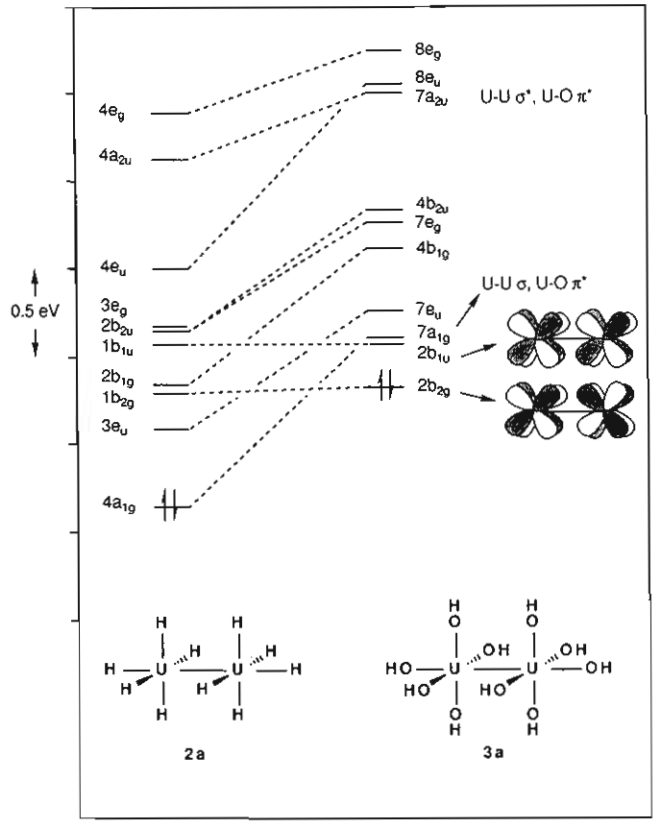

Figure 3. Comparative molecular orbital diagram of the f-block orbitals of **2a** and **3a**.

in a nodal plane of the former. However, these U–U orbitals represent significantly weaker U–U bonding than that found in the σ orbital of **2a**: at a U–U distance of 2.90 Å, the δ and δ^* orbitals are split by only 0.24 eV. The U–U σ bonding orbital in **3a** is destabilized by an antibonding interaction between the

Table V. Energies and Percent Characters of the f-Block Orbitals of **3b**

MO	ϵ, eV	type[a]	% U	% t-OH	% μ-OH
$7b_{2g}$	−4.97	ϕ^*/π^*	86	14	0
$8b_{3u}$	−5.12	ϕ/π	85	13	2
$10b_{1u}$	−5.18	δ^*/σ^*	83	9	8
$11a_g$	−5.44	δ/σ	88	9	3
$8b_{3g}$	−5.46	π^*/ϕ^*	87	10	3
$9b_{2u}$	−5.58	π/ϕ	87	9	4
$9b_{1u}$	−5.74	σ^*/δ^*	89	11	0
$7b_{3g}$	−5.97	π^*/ϕ^*	89	10	1
$4b_{1g}$	−6.14	δ	87	8	5
$8b_{2u}$	−6.17	π/ϕ	88	11	1
$3a_u$	−6.21	δ^*	92	8	0
$6b_{2g}$	−6.58	π^*/ϕ^*	100	0	0
$10a_g$	−6.59	σ/δ	93	7	0
$7b_{3u}$	−6.90	π/ϕ	100	0	0

[a] Refers to primary U–U interaction type.

equatorial OH π orbitals and the inner "doughnuts" of the U f_{z^3} orbitals, shown as

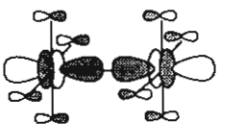

$7a_{1g}$ of **3a**

The destabilization of this strongly U–U bonding orbital pushes it above the δ and δ^* orbitals, and it is unoccupied. We are thus left with the conclusion that there is minimal U–U bonding in this unbridged, D_{4h} geometry of $U_2(OH)_{10}$.

Finally, the U–OH π bonding orbitals of **3a** (Table IV) reflect substantial 5f interaction in several levels. It is interesting to note that two OH π levels ($1a_{2g}$ and $1a_{1u}$) are entirely OH in character and are unable to interact with any U s, p, d, or f atomic orbitals in the D_{4h} geometry. The importance of this point will be addressed in the discussion of the D_{2h} conformation.

We now turn to the doubly bridged D_{2h} geometry of $U_2(OH)_{10}$ (**3b**). As in the σ-only system **2b**, the $U_2(OH)_{10}$ D_{2h} geometry can be derived from the D_{4h} geometry via a 45° rotation about the x axis of each atom. The frontier MO diagram of **2b** is depicted on the right half of Figure 2, and the energies and compositions of its U f-block and U–O π-bonding levels are listed in Tables V and VI, respectively. The three orbital sets of **2b** are energetically similar to those in **2a**. Like that of **2b**, the f block of **3b** contains greater mixing in the U–U interactions than in **3a**, as now σ/δ hybridization occurs along with π/ϕ mixing. As in **3a**, there is substantial OH π interaction in the 5f block of **3b**, which leads to destabilization of the U 5f-based orbitals. Figure 4 depicts a correlation of the U-based orbitals in **2b** and **3b**. Once again, all but two f-based orbitals ($6b_{2g}$ and $7b_{3u}$) of **3b** are significantly destabilized by OH π-antibonding interaction. The $6b_{2g}$ and $7b_{3u}$ orbitals comprise U–U π/ϕ and π^*/ϕ^* interactions, respectively, which under D_{2h} symmetry cannot interact with any ligand σ or π combination and hence are 100% U in character. The primarily U–U σ-type interaction ($10a_g$) is again destabilized

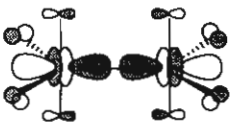

$10a_g$ of **3b**

by OH π interaction, such that it is pushed higher in energy than the U–U π/ϕ orbital and remains unoccupied. From this electronic description of the 5f block of **3b**, it is clear that the f^2 configuration of $U_2(O\text{-}i\text{-}Pr)_{10}$ (**1**) would not lead to any significant U–U bonding interaction, as reflected in the nonbonding U–U distance of 3.789 Å observed for **1**.

The composition of the U–O π-bonding orbitals of **3b** (Table VI) illustrates the extent of U character in these interactions, a

Table VI. Energies and Percent Characters of the U–O π Interactions of **3b**

MO	ϵ, eV	% U	% f	% d	% p	% s	% t-OH	% μ-OH
$5b_{2g}$	−9.17	2	28	3	69	0	98	0
$6b_{3u}$	−9.17	1	32	0	68	0	93	6
$3b_{1g}$	−9.23	2	96	4	0	0	82	16
$6b_{3g}$	−9.29	5	25	1	74	0	87	8
$7b_{2u}$	−9.38	6	72	2	26	0	93	1
$2a_u$	−9.41	8	96	4	0	0	92	0
$8b_{1u}$	−9.55	10	31	7	59	3	64	26
$5b_{3u}$	−9.88	5	18	16	66	0	47	48
$9a_g$	−9.93	9	52	9	38	1	89	2
$5b_{3g}$	−9.97	16	92	0	8	0	80	4
$6b_{2u}$	−10.05	15	93	1	6	0	85	0
$2b_{1g}$	−10.22	12	98	2	0	0	32	56
$7b_{1u}$	−10.32	16	74	22	3	1	78	6
$8a_g$	−10.37	15	71	28	1	0	85	0
$4b_{2g}$	−10.46	10	1	87	12	0	90	0
$1a_u$	−10.63	12	27	73	0	0	88	0
$6b_{1u}$	−10.68	19	71	16	4	9	32	49
$1b_{1g}$	−10.80	10	1	99	0	0	66	24
$4b_{3g}$	−10.96	24	77	14	9	0	14	62
$4b_{3u}$	−11.10	10	2	97	1	0	50	40

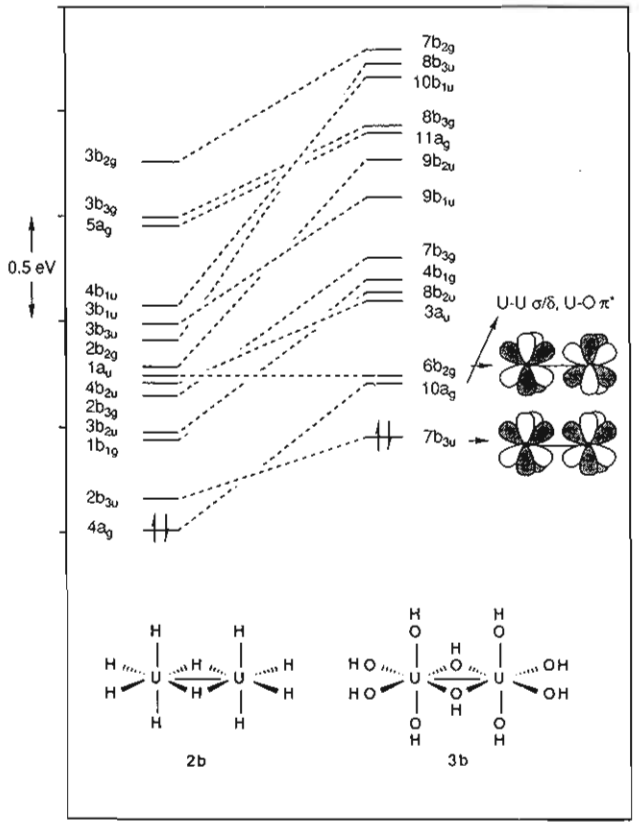

Figure 4. Comparative molecular orbital diagram of the f-block orbitals of **2b** and **3b**.

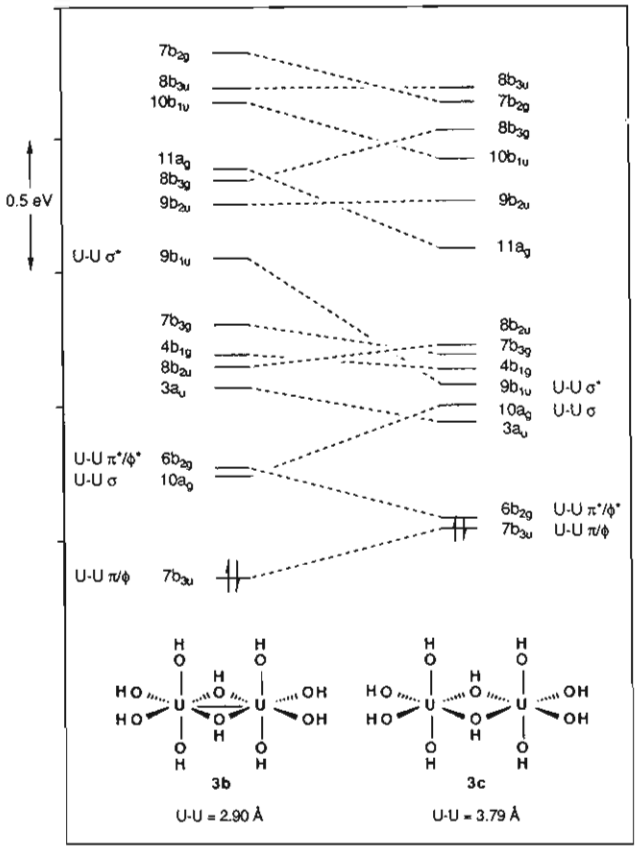

Figure 5. Comparative molecular orbital diagram correlating the energies of the f-block orbitals as the U–U separation is increased from 2.90 Å (**3b**) to 3.79 Å (**3c**).

large degree of which is contributed by the 5f orbitals. It is interesting to note that, in the D_{2h} geometry, *all of the OH π combinations are able to interact with uranium atomic orbitals.* Therefore, the desire for $U_2(O\text{-}i\text{-}Pr)_{10}$ to adopt a bridged D_{2h} geometry rather than an unsupported D_{4h} conformation appears to be 2-fold: First, and most important, the U–U bonding interactions are weak in these systems. Second, the U–OH π interactions are more favorable in the D_{2h} system than in the D_{4h} system.

Increasing the U–U separation in **3b** from 2.90 to 3.79 Å yields the model complex **3c**, the conformation of which reflects the actual structure of **1**. Lengthening the U–U distance affects the U–O σ- and π-bonding levels only slightly. The greatest changes are seen, not surprisingly, in the 5f-based orbitals. Figure 5 illustrates the effects of increasing the U–U separation from 2.90 to 3.79 Å on the 5f orbital energies. At 3.79 Å the U–U interactions are essentially negligible. For example, the splitting of the U–U σ and σ^* orbitals ($10a_g$, $9b_{1u}$) decreases from 0.85 eV at 2.90 Å to <0.1 eV at 3.79 Å. As a result, the ordering of the 5f-based orbitals in **3c** is due almost entirely to the effects of U–OH σ- and π-antibonding interactions. For this reason, the U–U π/ϕ and π^*/ϕ^* orbital set ($7b_{3u}$, $6b_{2g}$) which cannot interact with the ligand set, is stabilized with respect to the remainder of the f-block orbitals.

$Cp_2U_2O_4$. Given that there are still no characterized dinuclear actinide complexes that exhibit a significant actinide–actinide interaction, it is intriguing to speculate on possible ligand environments that will foster actinide–actinide bond formation. The simplest such bond would be a single bond formed by two f^1 U(V) centers. We have already seen that $U_2(OR)_{10}$ systems are disfavorable for U–U bond formation because of the significant destabilization of the U–U σ-bonding orbital by the alkoxide

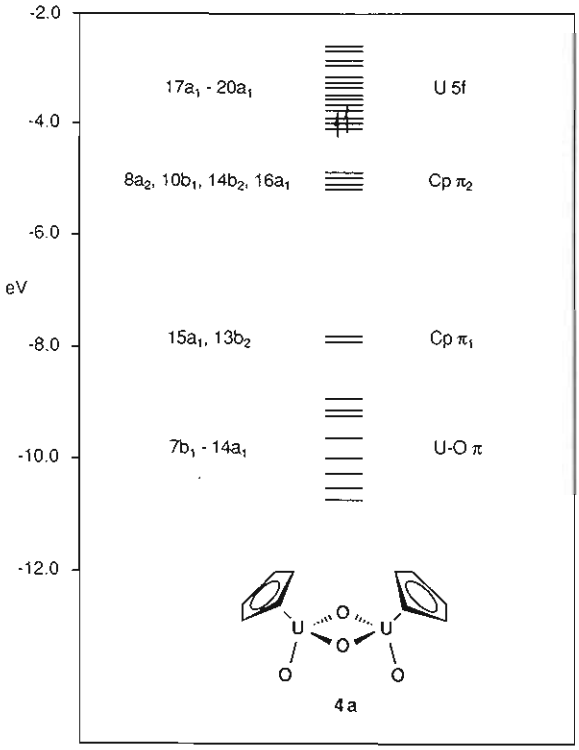

Figure 6. Molecular orbital diagram of the frontier valence orbitals of **4a** through the U 5f levels.

ligands. Here we will examine the bonding in a hypothetical U(V) dimer, $[CpUO]_2(\mu\text{-}O)_2$ (**4**; Cp = η^5-C_5H_5). We believe that a compound such as **4** offers several advantages over **1** with respect to U–U bond formation: (1) The shorter U–O distances associated with oxo ligands compared to alkoxide ligands could force the U atoms closer to one another without creating U–(μ-O)–U angles that are overly acute. (2) If it is assumed that each Cp ligand occupies three coordination sites, the ligand arrangement about each U atom is pseudooctahedral, so the analysis of systems **2** and **3** should be transferable to **4**. (3) The ligand environment in **4** has ample precedent in Cr, Mo, and W chemistry.[16] (4) The replacement of three alkoxide ligands with a Cp ligand on each U atom should mitigate the destabilization of the U–U σ interaction that was so prevalent in the $U_2(OH)_{10}$ system.

Three different assumed geometries were investigated for the $Cp_2U_2O_4$ system, each with a *cis*-Cp arrangement and C_{2v} symmetry. The model systems **4a** and **4b** can formally be considered

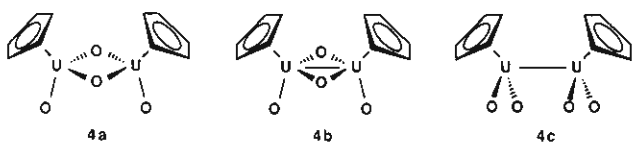

as edge-sharing bioctahedra, similar in geometry to **3c** and **3b**, respectively. In **4a**, an obtuse U–(μ-O)–U angle of 113.2° was used, yielding a long U–U separation of 3.34 Å, whereas in **4b** the U–(μ-O)-U angle was chosen to be 90.5°, affording a U–U distance of 2.84 Å. Structure **4c** was devised in order to examine the electronic nature of an unsupported U–U bond with this ligand set.

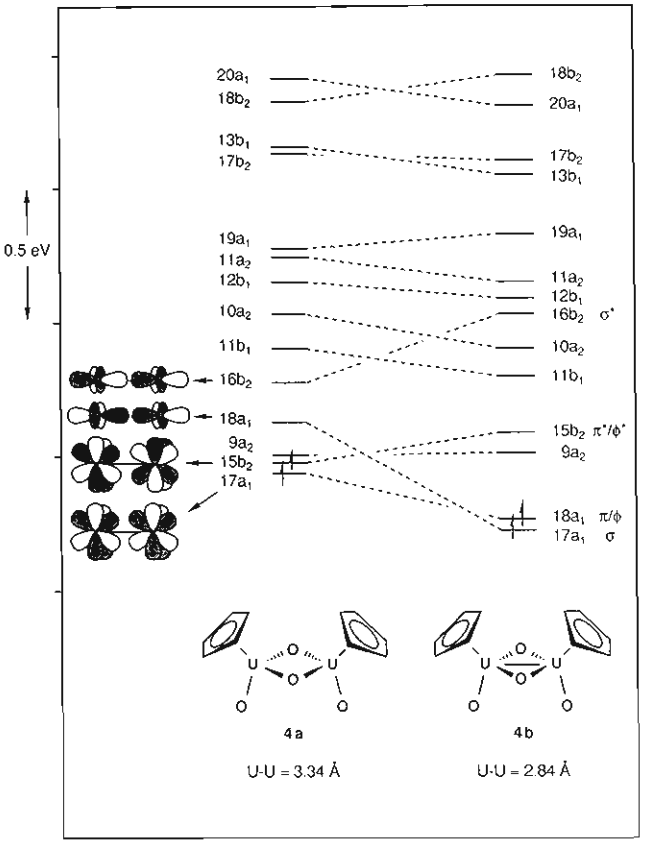

Figure 7. Comparative frontier orbital diagrams of the 5f-based orbitals of **4a** and **4b**.

The frontier molecular orbital diagram of **4a** is shown in Figure 6. As before, the highest energy frontier orbitals are a block of 14 uranium-based orbitals, primarily 5f in character. Below these are located the Cp π_2 and π_1 bonding orbitals. Lower in energy are the U–O π-bonding interactions. Table VII lists the energies and compositions of the orbitals constituting the f-block and U–O π interactions. Several aspects of the table are noteworthy: (1) The average percent metal character of the f-block orbitals is 91%, similar to that of the $U_2(OH)_{10}$ series. (2) The f block displays significantly more d character in several orbitals than was found for the $U_2(OH)_{10}$ series. (3) The average percent metal character of the U–O π-bonding orbitals is 21%, which is approximately twice the metal character than was found for the U–O π orbitals of $U_2(OH)_{10}$. This effect exemplifies the stronger π-donor ability of the oxo ligand as compared to the hydroxide ligand. (4) In contrast to the situation we have generally found in Cp–actinide complexes,[17] the f contribution to the metal character of the U–O π orbitals is greater than the d, p, and s contributions combined. The importance of these features will be addressed along with the examination of the alternative geometries.

With a U–U separation of 2.84 Å, structure **4b** provides an opportunity to examine the electronic effect of U–U bonding in this system. Not unexpectedly, the overall electronic structure of **4b** is essentially identical with that of **4a** except in the U 5f region. A comparison of the f blocks of **4a** and **4b** is given in Figure 7. When the U–U distance is decreased from 3.34 to 2.84 Å, a very interesting electronic effect develops. At the longer distance, the two lowest energy 5f-based orbitals ($17a_1$, $15b_2$) are a U–U $(\pi/\phi)/(\pi^*/\phi^*)$ set split by only 0.04 eV. Higher in energy is the primarily U–U σ/σ^* set ($18a_1$, $16b_2$). When the U–U

(16) Cr: Herberhold, M.; Kremnitz, W.; Razavi, A.; Schollhorn, H.; Thewalt, U. *Angew. Chem., Int. Ed. Engl.* **1985**, *24*, 601–602. Mo: (a) Cousins, M.; Green, M. L. H. *J. Chem. Soc.* **1964**, 1567–1572. (b) Couldwell, C.; Prout, K. *Acta Crystallogr.* **1978**, *B34*, 933–934. (c) Arzoumanian, H.; Baldy, A.; Pierrot, M.; Petrignani, J.-F. *J. Organomet. Chem.* **1985**, *294*, 327–331. (d) de Jesûs, E.; Vázquez de Miguel, A.; Royo, P.; Lanfredi, A. M. M.; Tiripicchio, A. *J. Chem. Soc., Dalton Trans.* **1990**, 2779–2784. W: Herrmann, W. A. *J. Organomet. Chem.* **1986**, *300*, 111–137 and references therein.

(17) (a) Bursten, B. E.; Fang, A. *J. Am. Chem. Soc.* **1983**, *105*, 6495–6496. (b) Bursten, B. E.; Fang, A. *Inorg. Chim. Acta* **1985**, *110*, 153–160. (c) Bursten, B. E.; Casarin, M.; DiBella, S.; Fang, A.; Fragalà, I. L. *Inorg. Chem.* **1985**, *24*, 2169–2173. (d) Bursten, B. E.; Strittmatter, R. J. *J. Am. Chem. Soc.* **1987**, *109*, 6606–6608. (e) Bursten, B. E.; Rhodes, L. F.; Strittmatter, R. J. *J. Am. Chem. Soc.* **1989**, *111*, 2758–2766. (f) Bursten, B. E.; Strittmatter, R. J. *Angew. Chem.*, in press.

Table VII. Energies and Percent Characters of Selected Orbitals of **4a**

MO	ϵ, eV	% U	% f	% d	% p	% s	% O	% Cp
$20a_1$	−2.59	82	92	8	0	0	8	10
$18b_2$	−2.66	87	85	8	2	5	9	4
$13b_1$	−2.85	83	93	7	0	0	8	9
$17b_2$	−2.85	85	93	6	0	1	6	9
$19a_1$	−3.23	94	87	11	0	2	4	2
$11a_2$	−3.24	90	89	11	0	0	3	7
$12b_1$	−3.30	89	99	1	0	0	10	1
$10a_2$	−3.48	87	97	2	1	0	4	9
$11b_1$	−3.61	93	95	5	0	0	3	4
$16b_2$	−3.73	97	97	3	0	0	2	1
$18a_1$	−3.88	96	99	1	0	0	2	2
$9a_2$	−4.02	98	99	1	0	0	0	2
$15b_2$[a]	−4.04	100	100	0	0	0	0	0
$17a_1$[a]	−4.08	98	100	0	0	0	1	1
$14a_1$	−8.91	16	52	23	25	0	83	1
$9b_1$	−9.20	15	89	6	5	0	84	1
$12b_1$	−9.25	19	29	28	17	26	47	34
$8b_1$	−9.65	18	78	22	0	0	82	0
$7a_2$	−9.95	24	39	45	16	0	76	0
$13a_1$	−10.24	27	17	44	26	13	63	10
$11b_2$	−10.56	28	70	15	5	10	71	1
$7b_1$	−10.74	20	48	47	5	0	80	0

[a] Highest occupied molecular orbital; occupation = 1.

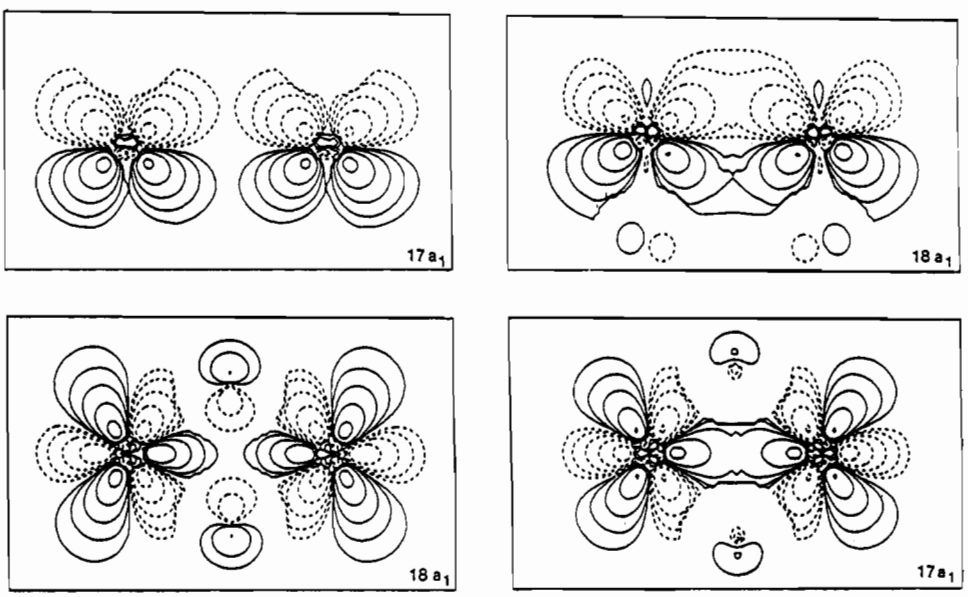

Figure 8. Contour diagrams of the $17a_1$ and $18a_1$ orbitals of **4a** and **4b**. The contour values used were ±0.02, ±0.04, ±0.08, ±0.16, and ±0.32.

distance is decreased to 2.84 Å, the U–U σ and (π/ϕ) orbitals, both of a_1 symmetry, are substantially stabilized and separated 0.37 eV from the next lowest 5f-based orbital. Contour plots of the $17a_1$ and $18a_1$ orbitals at U–U distances of 3.34 and 2.84 Å are shown in Figure 8. The U–U σ interaction is depicted in the plane that contains the bridging oxo ligands (xy plane), while the U–U (π/ϕ) interaction is shown in the plane containing the terminal oxo ligands, U atoms, and Cp centroids, perpendicular to the bridge plane (yz plane). It is seen that both interactions increase significantly upon the 0.5-Å reduction in the U–U distance. At 2.84 Å, the U–U (π/ϕ) set is split by 0.43 eV and the σ set by 0.98 eV. Because the $17a_1$ and $18a_1$ orbitals of **4b** are nearly degenerate, it does not seem likely to us that a diamagnetic complex with a fully occupied U–U σ-bonding MO would result, at least at the assumed U–U separationof 2.84 Å. More likely, **4b** would be paramagnetic with a $\sigma^1(\pi/\phi)^1$ ground electronic configuration, as shown in Figure 7. Such a configuration would lead to a U–U bond, albeit of only half the strength of a "true" U–U σ bond, held together primarily by the bridging oxo ligands. In other words, if a compound such as **4b** were prepared, these calculations suggest that it may be possible for the oxo ligands to form a strong enough U_2O_2 core to produce the unusual U–U bonding situation delineated above.

That the μ-oxo ligands play an important role in creating a favorable U–U bonding environment in $Cp_2U_2O_4$ is further emphasized in the electronic structure of the model unsupported complex, **4c**. The U–O and U–Cp bonding orbitals of **4c** are similar in both energy and composition to those of the bridging oxo geometries, **4a** and **4b**. Again, as is not unexpected, the f block displays significant deviations. Changing the oxo ligand arrangement from $(t\text{-}O)_2(\mu\text{-}O)_2$ to $(t\text{-}O)_4$ forces a rehybridization and reordering of the 5f-based levels. For **4c**, at a U–U distance of 2.84 Å, the lowest energy 5f-based orbital is a weak U–U δ interaction; the much stronger U–U σ-bonding MO is located 0.20 eV higher in energy. This interesting level ordering is *not* a consequence of reduced σ interaction between the $5f_{z^3}$ orbitals of the two uranium atoms. In fact, the σ/σ^* splitting in **4c** is 0.93 eV, similar to that found in **4b**, whereas the δ/δ^* splitting is only

Table VIII. Atomic Sphere Radii of the Atoms in Model Complexes **2–4**.

atom[a]	sphere radius, bohr	
	2a	**2b**
outer sphere	7.6207	7.1638
U	2.9678	2.9782
H(ax)	1.5357	1.5383
H(eq)	1.5282	1.5353
H(μ)		1.5968

atom[a]	sphere radius, bohr		
	3a	**3b**	**3c**
outer sphere	9.7883	9.0883	9.5626
U	2.7020	2.6854	2.6615
O(ax)	1.7889	1.7846	1.7896
H(ax)	1.1471	1.1468	1.1474
O(eq)	1.7901	1.7891	1.7836
H(eq)	1.1472	1.1472	1.1467
O(μ)	1.7907	1.7917	
H(μ)	1.1426	1.1446	

atom[a]	sphere radius, bohr		
	4a	**4b**	**4c**
outer sphere	10.2240	10.2240	10.5584
U	2.6340	2.6193	2.5780
O(t)	1.7550	1.7514	1.7515
O(μ)	1.7841	1.7894	
C	1.6978	1.6977	1.6976
H	1.2832	1.2832	1.2831

[a] ax = axial, eq = equatorial, μ = bridging, and t = terminal.

0.23 eV. Once again, the apparent energy reversal of the U–U σ and δ interactions is due to the destabilizing effect of the π-donor oxo ligands. The U–U σ and δ bonding orbitals of **4c** are depicted as

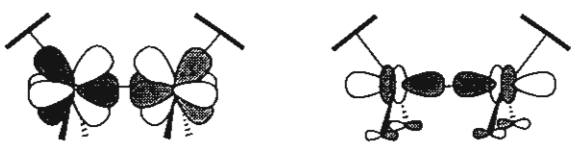

U-U δ U-U σ/U-O π^*

The δ orbital is unable to interact with the oxo σ or π orbitals and is therefore 100% U in character. On the other hand, the U–U σ orbital can interact with the oxo π orbitals and does so in an antibonding fashion. This serves to destabilize the U–U σ-bonding orbital and thus weaken the overall U–U bonding picture. Like the unbridged $U_2(OH)_{10}$ structure, the U–U bonding interactions in **4c** appear to be weak even at the comparatively short U–U distance investigated.

Conclusions

The calculations on species **2–4** suggest that it should be possible to construct a ligand environment that will allow two f^1 U(V) centers to form a direct U–U σ bond. Clearly, a homoleptic alkoxide complex, such as **1**, is not the route to direct uranium–uranium bonding; donation from the strong π-donor ligands in the edge-sharing bioctahedral geometry overpowers the 5f–5f interactions that are needed to form a U–U bond.

The model complex **4b** is one in which the disruption of the U–U bonding by the π-bonding ligand framework is greatly decreased relative to that in **3b**. There are other means by which this could be achieved, of course. A homoleptic alkyl dimer, U_2R_{10}, in either a bridged or unbridged geometry would have no ligand-to-metal π donation (ignoring weak hyperconjugative effects). Our calculations on **2a** and **2b** suggest that weak, but significant, U–U bonding would exist in either geometry. Unfortunately, homoleptic uranium alkyls are notoriously difficult to synthesize,[18] suggesting that π-donor ligands generally confer greater stability to uranium complexes. Amide ligands, which are strong π donors that only possess one π-donor orbital per ligand, may also be more effective at promoting U–U bond formation than alkoxide ligands, which have two π-donor orbitals per ligand. Clearly, we feel that the prospects for designing complexes that contain a U–U bond are promising. We hope that the theoretical studies presented here stimulate new synthetic approaches to this potentially very exciting class of compounds.

Acknowledgment. R.H.C. gratefully acknowledges support as an Indiana University Chester Davis Research Fellow and as an NSF Postdoctoral Fellow. This research was supported by the Division of Chemical Sciences, Office of Basic Energy Sciences, U.S. Department of Energy (Grant DE-FG02-86ER13529 to B.E.B.).

Appendix

The atomic coordinates used in the model systems **2a** and **2b** were constructed by assuming the following bond lengths: **2a**, U–H = 1.80 Å, U–U = 2.84 Å; **2b**, U–(t-H) = 1.80 Å, U–(μ-H) = 2.10 Å, U–U = 2.84 Å. Complexes **2a** and **2b** were idealized to D_{4h} and D_{2h} symmetry, respectively. The atomic coordinates used for **3b** were taken from the crystal structure of $U_2(O\text{-}i\text{-}Pr)_{10}$[6] with the following alterations: The *i*-Pr groups were replaced with H, assuming an O–H distance of 1.00 Å. The U–O–H angles for the terminal OH ligands were set at 180°. The structure was idealized to D_{2h} symmetry. The coordinates for **3a** were derived from those used for **3b** by reducing the U–U distance to 2.90 Å. The U–(t-O) and U–(μ-O) distances were the same as in **3b**, while the U–(μ-O)–U angle was necessarily decreased by the appropriate amount, retaining D_{2h} symmetry. The U–O and O–H distances used for **3c** were taken from the terminal OH ligands of **3b**. A U–U distance of 2.84 Å was used, and the molecule was idealized to D_{4h} symmetry. The atomic coordinates for the model compounds, **4a–c** were generated by assuming the following bond lengths: U–(t-O) = 1.75 Å, U–(μ-O) = 2.00 Å, U–C = 2.79 Å, C–C = 1.39 Å, C–H = 1.08 Å. The U–U–(t-O) and U–U–Cp(centroid) angles were set at 90 and 145°, respectively, with a cis-Cp geometry in each case. A (t-O)–U–(t-O) angle of 90° was assumed for **4c**. A U–U distances of 3.34 Å was used for **4a**, and 2.84 Å, for **4b** and **4c**. All three model complexes were idealized to C_{2v} symmetry.

All of the calculations reported here were carried out on an IBM 3081D computer and were undertaken with existing codes for the Xα scattered wave molecular orbital method. An initial molecular charge density and potential were constructed from a superposition of Herman–Skillman[19] neutral charge densities for U, O, C, and H. The α-exchange parameters were taken from Schwarz[20] with the uranium α value extrapolated to 0.692. A valence-electron weighted average of atomic α values was used for the inter- and outer-sphere regions. Overlapping atomic sphere radii were taken to be 89% of the atomic number radii in accordance with the nonempirical procedure of Norman.[21] The outer sphere was made tangential to the outermost atomic spheres. The sphere radii of the individual atoms in complexes **2–4** are summarized in Table VIII.

The symmetry-adapted linear combinations of atomic orbitals for all calculations included s, p, d, and f type spherical harmonics on the uranium atoms, s and p on carbon and oxygen atoms, s on hydrogen atoms, and spherical harmonics through $l = 4$ on the outer sphere. Core energy levels were never frozen; in each case they were calculated explicitly by using only the surrounding atomic sphere potential for the atom in question.

The calculations were converged to self-consistency by using the Wood and Boring formalism[12] to incorporate the relativistic effects from the outset. This was found to be a quicker and less expensive technique than first achieving a nonrelativistic converged potential and then gradually mixing in relativistic effects. Convergence was assumed when the maximum shift in the potential from one iteration to the next was less than 0.0010 Ry.

(18) Van Der Sluys, W. G.; Burns, C. J.; Sattelberger, A. P. *Organometallics* **1989**, *8*, 855–857.

(19) Herman, F.; Skillman, S. *Atomic Structure Calculations*; Prentice-Hall: Englewood Cliffs, N.J., 1963.

(20) Schwarz, K. *Phys. Rev. B* **1972**, *5*, 2466–2468.

(21) Norman, J. G., Jr. *Chem. Phys.* **1974**, *61*, 4630–4635.